Journal of Solid State Chemistry 181 (2008) 2964–2975

Contents lists available at ScienceDirect

Journal of Solid State Chemistry

journal homepage: www.elsevier.com/locate/jssc

On the system cerium–platinum–silicon

Alexander Gribanov [a,b,*], Andriy Grytsiv [a], Esmaeil Royanian [c], Peter Rogl [a], Ernst Bauer [c], Gerald Giester [d], Yurii Seropegin [b]

[a] Institute of Physical Chemistry, University of Vienna, Währingerstrasse 42, Wien A-1090, Austria
[b] Chemistry Department of the Moscow State University, Leninskie Gory, GSP-1, Moscow 119991, Russia
[c] Institute of Solid State Physics, Vienna University of Technology, A-1040 Wien, Wiedner Hauptstr. 8-10, Austria
[d] Institute of Mineralogy and Crystallography, University of Vienna, Althanstrasse 14, Wien A-1090, Austria

ARTICLE INFO

Article history:
Received 19 May 2008
Received in revised form
1 July 2008
Accepted 13 July 2008
Available online 20 July 2008

Keywords:
Ternary system Ce–Pt–Si
Ternary silicides
Phase equilibria at 800 °C
Single-crystal and X-ray powder diffraction

ABSTRACT

Phase relations in the ternary system Ce–Pt–Si have been established for the isothermal section at 800 °C based on X-ray powder diffraction, metallography, scanning electron microscopy (SEM) and electron probe microanalysis (EPMA) techniques on about 120 alloys, which were prepared by various methods employing arc-melting under argon or powder reaction sintering. Nineteen ternary compounds were observed. Atom order in the crystal structures of τ_{18}-$Ce_5(Pt,Si)_4$ (*Pnma*; $a = 0.77223(3)$ nm, $b = 1.53279(8)$ nm $c = 0.80054(5)$ nm), τ_3-$Ce_2Pt_7Si_4$ (*Pnma*; $a = 1.96335(8)$ nm, $b = 0.40361(4)$ nm, $c = 1.12240(6)$ nm) and τ_{10}-$CePtSi_2$ (*Cmcm*; $a = 0.42943(2)$ nm, $b = 1.67357(5)$ nm, $c = 0.42372(2)$ nm) was determined by direct methods from X-ray single-crystal CCD data and found to be isotypic with the Sm_5Ge_4-type, the $Ce_2Pt_7Ge_4$-type and the $CeNiSi_2$-type, respectively. Rietveld refinements established the atom arrangement in the structures of Pt_3Si (Pt_3Ge-type, *C2/m*, $a = 0.7724(2)$ nm, $b = 0.7767(2)$ nm, $c = 0.5390(2)$ nm, $\beta = 133.86(2)^\circ$), τ_{16}-Ce_3Pt_5Si (Ce_3Pd_5Si-type, *Imma*, $a = 0.74025(8)$ nm, $b = 1.2951(2)$ nm, $c = 0.7508(1)$ nm) and τ_{17}-Ce_3PtSi_3 ($Ba_3Al_2Ge_2$-type, *Immm*, $a = 0.41065(5)$ nm, $b = 0.43221(5)$ nm, $c = 1.8375(3)$ nm). Phase equilibria in Ce–Pt–Si are characterised by the absence of cerium solubility in platinum silicides. Cerium silicides and cerium platinides, however, dissolve significant amounts of the third component, whereby random substitution of the almost equally sized atom species platinum and silicon is reflected in extended homogeneous regions at constant Ce content such as for τ_{13}-$Ce(Pt_xSi_{1-x})_2$, τ_6-$Ce_2Pt_{3+x}Si_{5-x}$ or τ_7-$CePt_{2-x}Si_{2+x}$.

1. Introduction

Besides the fact that many compounds from the Ce–Pt–Si system exhibit interesting electrical and/or magnetic properties such as heavy-fermion behavior in CePtSi [1–5] and $CePtSi_2$ [6–8] and/or Kondo-lattice behavior in $CePtSi_2$ [6–8] and $CePt_2Si_2$ [9–13], it was particularly the discovery of $CePt_3Si$ as the first non-centrosymmetric heavy-fermion superconductor [14,15], which has stimulated high interest in the physical properties of $CePt_3Si$ [16–22] and Ce–Pt–Si compounds [23–25]. Crystal growth and bulk material syntheses require detailed knowledge of phase relations as well as of crystal structures. A critical assessment [26] summarized all data available then on the Ce–Pt–Si system with respect to phase equilibria [27] incorporating also unpublished data [28] and knowledge on physical properties. As a result of the critical review, an isothermal section at 600 °C was presented, which however, left many regions in the diagram with dashed tie-lines open for further studies. Therefore a reinvestigation of the phase relations became the subject of the present work. In order to profit from enhanced diffusion in the system combining elements with rather different melting points, a temperature of 800 °C was chosen for the isothermal section.

2. Experimental techniques

More than 120 alloys, each with a weight of 1 g, were prepared by argon arc-melting from high-purity elements (more than 99.9 mass%), on a water-cooled copper hearth. To ensure complete fusion, all alloys were re-melted three times. Part of each sample was vacuum-sealed in a quartz tube and annealed at 800 °C for 15–90 days before being quenched in cold water. The equilibrium state of the samples was carefully monitored by metallography, electron probe microanalysis (EPMA) and X-ray diffraction (XRD) techniques. Alloys, which even after long-term annealing did not reach equilibrium, were subjected to a cascaded heat treatment at

* Corresponding author at: Chemistry Department of the Moscow State University, Leninskie Gory, GSP-1, Moscow 119991, Russia. Fax: +7 495 939 0171.
E-mail addresses: avgri@mail.ru, grav@general.chem.msu.ru (A. Gribanov).

0022-4596/$ - see front matter © 2008 Elsevier Inc. All rights reserved.
doi:10.1016/j.jssc.2008.07.010

1100, 1000, 900 and finally 800 °C in order to accelerate reaction kinetics. In several cases the samples in addition were powderised, cold compacted and sintered at 800 °C for 2 weeks.

X-ray powder diffraction data from as-cast and annealed alloys were collected employing a Guinier–Huber image plate system with Cu-$K\alpha$1-radiation ($8^\circ < 2\theta < 100^\circ$). Precise lattice parameters were calibrated against Ge as internal standard ($a_{Ge} = 0.565754$ nm [29]) using program STOE-WinXpow [30].

Single crystals were mechanically isolated from crushed alloys. Inspection on an AXS-GADDS texture goniometer assured high crystal quality, unit cell dimensions and Laue symmetry of the specimens prior to X-ray intensity data collection on a four-circle Nonius Kappa diffractometer equipped with a CCD area detector and employing graphite monochromated Mo$K\alpha$ radiation ($\lambda = 0.071073$ nm). Orientation matrix and unit cell parameters were derived using program DENZO [31]. No absorption corrections were necessary because of the rather regular crystal shape and small dimensions of the investigated specimens. The structures were solved by direct methods [32] and refined with the SHELXL-97 program [33]. Quantitative Rietveld refinements were performed with the FULLPROF program [34,35], employing internal tables or X-ray atomic form factors. For search of minority phases as well as for quantitative structure refinements powder patterns with maximum intensity of more than 20,000 counts were taken. Atom parameters were standardized with the aid of program STRUCTURE TIDY [36].

All as-cast and annealed samples were polished via standard procedures and have been examined by optical metallography and scanning electron microscopy (SEM). Specimen compositions were determined by EPMA on a Carl Zeiss DSM 962 instrument equipped with a Link EDX system operated at 20 kV and 60 μA. As external standards we used pure elements Pt, Si as well as binary and ternary compounds of defined composition, which were also backed by single-crystal refinement; Pt_3Si, Pt_2Si, Pt_6Si_5, CeSi, $CePtSi_3$, $CePtSi_2$, $CePt_2Si$, $CePt_3Si$, $Ce_2Pt_7Si_4$ and Ce_3Pt_5Si. Although standard deviations of EPMA phase measurements were generally better than 0.3 at%, the average values obtained after correction have a confidence level of about 0.5 at%.

3. Binary systems

The binary system Ce–Pt is used in the version of Massalski [37]. The melting temperature of Ce_7Pt_3, however, was re-measured in a DTA experiment and found to be 860 °C [38]. The Ce–Si system was taken from a recent investigation [39]. There is no doubt about the formation of an additional phase, Ce_2Si_{3-x} ($CeSi_{1.34}$), for which crystal and magnetic structure were determined [40]. The investigation of the Pt–Si system by Massara and Feschotte [41] superseded the Pt–Si diagram presented in Massalski [37] and two more compounds, $Pt_{25}Si_7$ and $Pt_{17}Si_8$, were discovered from DTA analyses of about 110 alloys. X-ray data, however, were merely used to identify changes in the intensity patterns and no details were given on the crystal structures of the binary compounds. From a comparison of the phase diagram of Gohle and Schubert [42] with the version of Massara and Feschotte [41] the compound $Pt_{12}Si_5$ [43,44], appears to be shifted to composition Pt_5Si_2. In order to eliminate contradicting information in literature on formation and crystal structure of Pt–Si compounds, several alloys with compositions Pt_6Si_5, Pt_2Si, $Pt_{17}Si_8$, $Pt_{12}Si_5$, Pt_3Si, $Pt_{25}Si_7$ were studied by means of X-ray powder diffraction in as-cast state and after annealing at 800 °C. Our Rietveld refinements confirm structural details for PtSi, Pt_6Si_5, Pt_2Si (for both the low- and high-temperature modification) whilst significant disagreement was noticed for the atom positions of Pt_3Si (Pt_3Ge-type structure [42]) (see Section 4.2). Structural parameters reported for $Pt_{12}Si_5$ ($Pt_{12}Si_5$-type [43,45]) show significant differences between calculated and observed X-ray intensities. Furthermore, Pt_3Si (Fe_3C-type), $Pt_{17}Si_8$ and $Pt_{25}Si_7$ were not observed in the investigated alloys: the X-ray powder diffraction spectrum recorded from an alloy with composition $Pt_{17}Si_8$ was indexed as a mixture of Pt_2Si and "$Pt_{12}Si_5$" and similarly the alloy $Pt_{25}Si_7$ consists of Pt_3Si and (Pt). Consequently, the phase relations derived from the present investigation at 800 °C were found to be consistent with those reported by Massalski [37]. Crystallographic and melting data pertinent to the Ce–Pt–Si system are given in Table 1.

4. Results and discussion

4.1. Phase relations; the isothermal section Ce–Pt–Si at 800 °C

Phase relations in the ternary system at 800 °C are shown in Fig. 1. The most striking difference to the equilibria at 600 °C presented earlier [26,27] is the larger number of ternary phases as well as the absence of a significant solubility for silicon throughout the full homogeneity region of the binary compound $Ce(Ce_{1-x}Pt_x)Pt_4$. Furthermore, phase equilibria are characterized by the absence of cerium solubility in the various platinum silicides. However, mutual solubilities among cerium silicides and cerium platinides are significant. The essentially random substitution of the almost equally sized atom species platinum and silicon is reflected in extended homogeneous regions at constant Ce content for several binary and ternary compounds such as for τ_{13}-$Ce(Pt_xSi_{1-x})_2$, τ_6-$Ce_2Pt_{3+x}Si_{5-x}$ or τ_7-$CePt_{2-x}Si_{2+x}$. Data on the solubility and extension of the ternary homogeneity regions at 800 °C are included in Table 1. Composition and lattice parameters for phases involved in three-phase equilibria at 800 °C are listed in Table 2.

It has to be noted, that in addition to the ternary phases listed in Table 1, compounds with compositions $Ce_{30}Pt_{40}Si_{30}$ and $Ce_{22}Pt_{46}Si_{22}$ (at%) were detected with structures still unknown; however, these phases do not participate in phase equilibria at 800 °C.

4.2. Determination of crystal structures

Crystal structures for all those ternary compounds, which were already reported earlier, were found to be consistent with data in literature. For a series of new compounds crystal structures were derived either by single-crystal X-ray diffractometry or by Rietveld analyses and crystal data are summarized below and in Tables 3 and 4. Structural chemistry of the new compounds and solution phases follows in all cases the characteristics already outlined for the prototype structures. Interatomic distances agree well with the sum of metal radii of the elements.

4.2.1. The crystal structure of τ_{18}-$Ce_5(Pt_{0.12}Si_{0.88})_4$ with Sm_5Ge_4-type

Binary Ce_5Si_4 is known to crystallize with the tetragonal Zr_5Si_4-type structure [39,46]. EPMA data in Table 2 indicate that solubility of Pt at 800 °C proceeds up to 4.6 at% Pt beyond which on rising Pt content a narrow two-phase region of about 3 at% is formed connecting to a ternary phase, τ_{18} (Fig. 2a), with an extended homogeneity region up to 15 at% Pt. A single crystal, broken from an alloy with composition $Ce_{55.5}Pt_{5.3}Si_{39.2}$ (nominal composition in at%) within the τ_{18} region, revealed orthorhombic symmetry with space group *Pnma* and lattice parameters: $a = 0.77223(3)$ nm, $b = 1.53279(8)$ nm, $c = 0.80054(5)$ nm. The structure was solved by direct methods yielding a partial random distribution of Pt and Si sites fully compatible and isotypic with

Table 1
Crystallographic data of solid phases in the Ce–Pt–Si system

Phase/temperature	Space group	Lattice parameters (nm)			Comments
Range (°C)	Prototype	*a*	*b*	*c*	
(δCe) 798–726 [37]	$Im\bar{3}m$ W	0.412			[37]
(γCe) 726–61 [37]	$Fm\bar{3}m$ Cu	0.51610			[37]
(βCe) 61–(−177) [37]	$P6_3/mmc$ αLa	0.36810		1.1857	[37]
(αCe) <−177 [37]	$Fm\bar{3}m$ Cu	0.485			[37]
(Pt) <1769 [37]	$Fm\bar{3}m$ Cu	0.39236			[37]
(Si) <1414 [37]	$Fd\bar{3}m$ C (diamond)	0.54306			[37]
Ce_5Si_3 <1260 [39] $Ce_5(Si_{1-x}Pt_x)_3$	$I4/mcm$ Cr_5B_3	0.7868 0.7878 0.7855(2)		1.373 1.367 1.3850(5)	[46] [39] $x_{max} = 0.3$ [this work]
Ce_3Si_2 <1335 [39] $Ce_3(Si_{1-x}Pt_x)_2$	$P4/mbm$ U_3Si_2	0.7780 0.77870(6)		0.4367 0.43824(6)	[39] $x_{max} = 0.105$ [this work]
Ce_5Si_4 <1500 [39] $Ce_5(Si_{1-x}Pt_x)_4$	$P4_12_12$, Zr_5Si_4	0.7936 0.79669(6)		1.5029 1.4948(2)	[39] $x_{max} = 0.104$ [this work]
CeSi <1630 [39] $CeSi_{1-x}Pt_x$	$Pnma$, FeB	0.8298 0.8254(1)	0.3961 0.39997(7)	0.5959 0.59452(9)	[39] $x_{max} = 0.074$ [this work]
Ce_2Si_{3-x}	$Cmcm$ V_2B_3	0.44035	2.48389	0.39517	$x = 0.32$ [39]
$CeSi_{1.67}$ <1725 [39]	$Imma$ $GdSi_{2-x}$	0.4109	0.4189	1.3917	At 62.6 at% Si [39]
$CeSi_{2-x}$ <1575 [39] $Ce(Si_{1-y}Pt_y)_{2-x}$	$I4_1/amd$ $ThSi_2$	0.4192 0.42112(4) 0.4205(2)		1.3913 1.4019(2) 1.4082(7)	$x = 0$ [39] $y = 0.12$ [this work] $y_{max} = 0.148$ [this work]
Ce_7Pt_3 <975 [37] <860 [38] $Ce_7(Pt_{1-x}Si_x)_3$	$P6_3mc$ Th_7Fe_3	1.0204 1.02005 1.0251(2)		0.6399 0.63999 0.6380(2)	[46] [38] $x_{max} = 0.157$ [this work]
Ce_3Pt_2 <1200 [37] $Ce_3(Pt_{1-x}Si_x)_2$	$R\bar{3}$ Er_3Ni_2	0.8981 0.8976(2)		1.7078 1.7124(3)	[46] $x_{max} = 0.065$ [this work]
CePt <1800 [37] $CePt_{1-x}Si_x$	$Cmcm$ CrB	0.3918 0.3974(1)	1.0908 1.0940(4)	0.4527 0.4479(1)	[46] $x_{max} = 0.12$ [this work]
Ce_3Pt_4 <1600 [37]	$R\bar{3}$ Pu_3Pd_4	1.3657 1.3661(7)		0.5781 0.5779(3)	[46] [this work]
$Ce(Ce_{1-x}Pt_x)Pt_4$ <2200 [37]	$Fd\bar{3}m$ $MgCu_2$	 0.7745 0.77172 0.77286(3)			$0 \leqslant x \leqslant 0.5$ [37,48] $x = 0$ (300 K) [48] $x = 0$ (13 K) [48] $x = 0.09$ [this work]
	$F\bar{4}3m$ $AuBe_5$	0.7673 0.76380			$x = 0.5$ (300 K) [48] $x = 0.5$ (13 K) [48]
$CePt_5$ <1800 [37]	$P6/mmm$ $CaCu_5$	0.53685		0.43830	[46]
$Ce(Pt_{1-x}Si_x)_5$		0.5348(6)		0.4364(5)	$x_{max} = 0.103$ [this work]
$Pt_{25}Si_7$[a] <842 [41]	Unknown				[41]
Pt_3Si-ht[a] <846–440 [41]	$Pnma$ Fe_3C	0.5579	0.7697	0.5520	At 605 °C [44]
Pt_3Si-rt <440 [41]	$C2/m$ Pt_3Ge	0.7702 0.7724(2)	0.7765 $\beta = 133.813$ 0.7767(2) $\beta = 133.86(2)$	0.5378 0.5390(2)	[42] Binary Pt_3Si [this work]

Table 1 (*continued*)

Phase/temperature	Space group	Lattice parameters (nm)			Comments
Range (°C)	Prototype	*a*	*b*	*c*	
		0.7723(2)	0.7771(1) 133.85(1)	0.53902(7)	In $Ce_8Pt_{81}Si_{11}$ [this work]
		0.7725(2)	0.7770(1) 133.86(1)	0.53898(9)	In $Ce_8Pt_{78.5}Si_{13.5}$ [this work]
$Pt_{12}Si_5$-ht[b] (Pt_5Si_2-ht)	*P4/n*	1.3404		0.5451	[43] [41]
986–280 [43]	$Pt_{12}Si_5$	1.34055(5) 1.33996(7)		0.55186(3) 0.55142(4)	Binary $Pt_{12}Si_5$ [this work][b] In $Ce_4Pt_{70}Si_{26}$ [this work][b]
$Pt_{12}Si_5$–rt[a] (Pt_5Si_2–rt)	*I4/m*	0.9753		0.5537	At 792 °C [44] [41]
<280 [43]	$Ni_{12}P_5$	0.9607		0.5542	At 902 °C [44]
$Pt_{17}Si_8$-ht[a] <1003–770	Unknown				[41]
$Pt_{17}Si_8$-rt[a] <770 [41]	Unknown				[41]
Pt_2Si-ht <1118–745 [41]	$P\bar{6}2m$ Fe_2P	0.6436 0.6525 0.6440 0.64567(9)		0.3569 0.3603 0.3573 0.35772(5)	[49] At 802 °C [44] [42] In $Ce_2Pt_{58}Si_{40}$ [this work]
Pt_2Si–rt <745 [41]	*I4/mmm* ThH_2	0.3933 0.3948 0.39310(2) 0.39312(4)		0.5910 0.5963 0.59231(4) 0.59259(9)	[42] At 603 °C [44] Binary Pt_2Si [this work] In $Pt_{70.6}Si_{29.4}$ [this work]
Pt_6Si_5 <1023 [41]	*P2₁/m* Pt_6Si_5	0.6169 0.6158(2) 0.61570(7)	0.3499 $\beta = 93.68$ 0.34915(7) $\beta = 93.59(2)$ 0.34890(4) $\beta = 93.576(9)$	1.5462 1.5425(3) 1.5425(1)	[42] Binary Pt_6Si_5 [this work] In $Ce_2Pt_{58}Si_{40}$ [this work]
PtSi <1238 [41]	*Pnma* MnP	0.5577 0.5595 0.55828(4)	0.3587 0.3603 0.35942(3)	0.5916 0.5932 0.59245(5)	[50] [46] In $Ce_{15}Pt_{40}Si_{45}$ [this work]
τ_1, $Ce_3Pt_{23}Si_{11}$ <1290 [27]	$Fm\bar{3}m$ $Ce_3Pt_{23}Si_{11}$	1.6837 1.6821 1.68647(5)			[51] SC data [27] [this work]
τ_2	Unknown				~$Ce_9Pt_{72}Si_{19}$ [this work]
τ_3, $Ce_2Pt_7Si_4$	*Pnma*	1.96335(2)	0.40361(1)	1.12240(2)	SC data [this work]
	$Ce_2Pt_7Ge_4$	1.9630(3)	0.40382(7)	1.1225(2)	[this work]
τ_4	Unknown				~$Ce_{18}Pt_{71}Si_{11}$ [this work]
τ_5, $CePtSi_3$ <1245 [27]	*I4mm* $BaNiSn_3$	0.4284 0.43215 0.43222(1)		0.9561 0.96075 0.96017(5)	[27] [23] [this work]
τ_6, $Ce_2Pt_{3+x}Si_{5-x}$	*Ibam* $U_2Co_3Si_5$	1.0061 0.9966(6) 0.9956(1)	1.1766 1.1663(8) 1.16526(1)	0.61323 0.6062(3) 0.60693(7)	[24] $x_{max} = 0.38$ [this work] $x_{min} = -0.09$ [this work]
τ_7, $CePt_{2-x}Si_{2+x}$ <1670 [27]	*P4/nmm* $CaBe_2Ge_2$	0.4252 0.4231 0.4253 0.42550(3) 0.42441(2)		0.9788 0.9844 0.9793 0.9795(1) 0.98341(7)	[52] $x = 0$ [27] $x = 0$ [25] $x = -0.055$ (min) [this work] $x = 0.12$ (max) [this work]
	P4mm or *P4*[c] $CePt_2Si_2$	0.42519		0.97951	$x = 0$ [10]
	I4/mmm $ThCr_2Si_2$	0.4246		0.9837	$x = 0$ [53]
τ_8, $CePt_3Si$ <1390 [27]	*P4mm* $CePt_3B$	0.40722 0.40786(4)		0.54423 0.54475(4)	[54] SC data [this work]
τ_9	Unknown				~$Ce_{23}Pt_{23}Si_{54}$ [this work]
τ_{10}, $CePtSi_2$	*Cmcm* $CeNiSi_2$	0.4288 0.4277 0.42943(2) 0.42908(3)	1.6718 1.6698 1.67357(5) 1.6739(2)	0.4238 0.4228 0.42372(2) 0.42371(5)	[6] [27] SC data [this work] [this work]
τ_{11}, $CePt_2Si$	*Cmcm* Inverse-$CeNiSi_2$	0.41067	1.8079	0.41821	[27]

Table 1 (*continued*)

Phase/temperature	Space group	Lattice parameters (nm)			Comments
Range (°C)	Prototype	*a*	*b*	*c*	
<1440 [28]		0.41008(4)	1.8046(2)	0.41734(4)	[this work]
τ_{12}	Unknown				~$Ce_{22}Pt_{67}Si_{11}$[this work]
τ_{13}, $Ce(Pt_xSi_{1-x})_2$	*P6/mmm*	0.41344		0.42868	$x = 0.3$ [28]
<1830 [27]	AlB_2	0.40960(4)		0.43130(3)	$x_{min} = 0.202$ [this work]
		0.41560(1)		0.42535(8)	$x_{max} = 0.34$ [this work]
	P6/mmm	0.8250		0.4332	$x = 0.25$ [55]
	Er_2RhSi_3				
τ_{14}, $CePt_{1-x}Si_{1+x}$	$I4_1md$	0.41982		1.4488	[56]
<1740 [27]	LaPtSi	0.41973		1.4498	[27]
		0.4206(1)		1.4490(3)	$x_{min} = 0$ [this work]
		0.41866 (2)		1.44914(8)	$x_{max} = 0.2$ [this work]
τ_{15}	Unknown				~$Ce_{33}Pt_{44}Si_{22}$ [this work]
τ_{16}, Ce_3Pt_5Si	*Imma*	0.74025(8)	1.2951(2)	0.7508(1)	[this work]
<1220 [28]	Ce_3Pd_5Si				
τ_{17}, Ce_3PtSi_3	*Immm*	0.41065(5)	0.43221(5)	1.8375(3)	[this work]
<1510 [28]	$Ba_3Al_2Ge_2$				
τ_{18}, $Ce_5(Pt_{1-x}Si_x)_4$	*Pnma*	0.77223(2)	1.53279(3)	0.80054(2)	SC data [this work]
	Gd_5Si_4	0.7643(1)	1.5330(3)	0.8007(2)	$x_{min} = 0.718$ [this work]
		0.7678(2)	1.5315(4)	0.8005(2)	$x = 0.819$ [this work]
		0.7704(2)	1.5321(4)	0.8000(3)	$x_{max} = 0.851$ [this work]
τ_{19}	Unknown				~$Ce_{55}Pt_{33}Si_{12}$ From 10.1 to 14.3 at % Si [this work]

[a] Phase was not observed in the present work in alloys annealed at 800 °C.
[b] Crystal structure is not confirmed, unit cell parameters are given for the crystal structure reported [43].
[c] A small deviation from $CaBe_2Ge_2$-type was noticed by Hiebl et al. [10] (weak reflections violating extinction rule $h+k = 2n+1$).

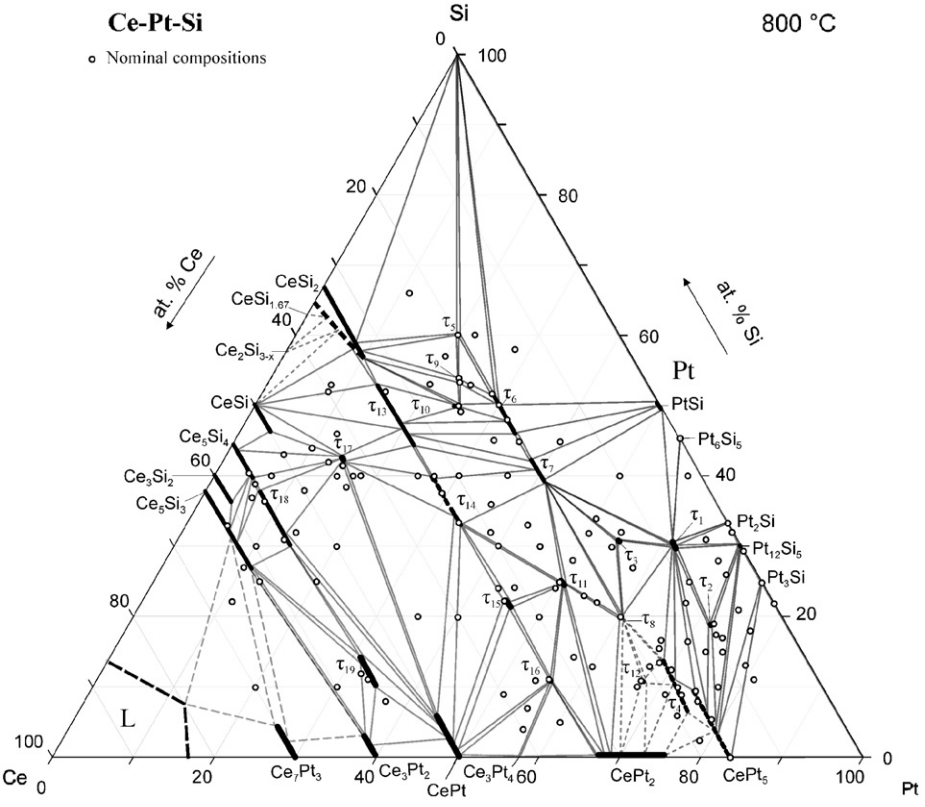

Fig. 1. System Ce–Pt–Si, isothermal section at 800 °C.

Table 2
Composition (standard deviation < 0.4 at%) and lattice parameters for phases from three phases regions of the Ce–Pt–Si system at 800 °C

Three phase field	Phase	EPMA			Lattice parameters (nm)		
		Ce	Pt	Si	*a*	*b*	*c*
τ_5+(Si)+$CeSi_2$	τ_5	20.0	19.4	60.6	0.43222(1)	–	0.96017(5)
	(Si)	0.0	0.0	100.0	0.54298(7)	–	–
	$CeSi_2$	32.9	8.0	59.1	0.42112(4)	–	1.4019(2)
τ_{10}+τ_9+$CeSi_2$	τ_{10}	24.8	25.1	50.1	0.42984(5)	1.6722(2)	0.42295(7)
	τ_9	22.9	23.0	54.1	Unknown	–	–
	$CeSi_2$	33.3	9.9	56.8	0.4205(2)	–	1.4082(7)
τ_{10}+τ_6+τ_9	τ_{10}	24.9	24.1	51.0	0.4282(2)	1.6743(5)	0.4253(2)
	τ_6	19.8	29.4	50.8	0.9956(1)	1.16526(1)	0.60693(7)
	τ_9	23.2	22.9	53.9	Unknown	–	–
τ_5+τ_6+τ_9	τ_5	19.8	20.2	60.0	0.4312(2)	–	0.9606(5)
	τ_6	19.8	29.3	50.9	0.9956(1)	1.16526(1)	0.60693(7)
	τ_9	23.0	22.8	54.2	Unknown	–	–
τ_5+τ_6+(Si)	τ_5	20.1	19.8	60.1	0.43168(3)	–	0.9599(1)
	τ_6	19.7	28.1	52.2	0.9942(1)	1.1645(1)	0.6065(1)
	(Si)	0.0	0.0	100.0	0.5427(1)	–	–
τ_6+(Si)+PtSi	τ_6	20.0	30.0	50.0	0.9934(7)	1.1679(8)	0.6056(4)
	(Si)	0.0	0.2	99.8	0.5431(1)	–	-
	PtSi	0.1	49.1	50.8	0.5576(1)	0.35835(6)	0.59358(7)
τ_6+τ_7+PtSi	τ_6	19.8	34.0	46.2	0.9966(6)	1.1663(8)	0.6062(3)
	τ_7	19.8	37.8	42.4	0.42441(2)	–	0.98341(7)
	PtSi	0.3	49.0	50.7	0.55828(4)	0.359542(3)	0.59245(5)
τ_1+τ_7+PtSi	τ_1	8.4	61.1	30.5	1.6872(3)	–	–
	τ_7	19.9	40.6	39.4	0.42580(5)	–	0.9792(2)
	PtSi	0.3	50.3	49.4	0.5574(9)	0.35822(7)	0.5937(1)
PtSi+Pt_6Si_5+τ_1	PtSi				0.5574(9)	0.35822(7)	0.5937(1)
	Pt_6Si_5				0.61570(7)	0.34890(4)	1.5425(1)
						$\beta = 93.576(9)^\circ$	
	τ_1				1.6872(3)	–	–
$PtSi_5$+Pt_2Si+τ_1	Pt_6Si_5	0.1	54.2	45.7	0.61570(7)	0.34890(4)	1.5425(1)
						$\beta = 93.576(9)^\circ$	
	Pt_2Si	0.3	66.3	33.4	0.64567(9)	–	0.35772(5)
	τ_1	7.9	61.8	30.3	1.6858(1)	–	–
τ_1+τ_2+$Pt_{12}Si_5$	τ_1	8.0	62.3	29.7	1.68808(6)	–	–
	τ_2	9.1	72.4	18.5	Unknown	–	–
	$Pt_{12}Si_5$	0.5	69.7	29.9	1.340(1)	–	0.5521(8)
τ_2+$CePt_5$+$Pt_{12}Si_5$	τ_2	8.9	72.4	18.7	Unknown	–	–
	$CePt_5$	15.8	79.2	5.0	0.5368(6)	–	0.4381(5)
	$Pt_{12}Si_5$	0.5	69.5	30.0	1.33996(7)	–	0.55142(4)
$CePt_5$+$Pt_{12}Si_5$+Pt_3Si	$CePt_5$	16.4	79.6	4.0	0.5364(6)	–	0.4388(3)
	$Pt_{12}Si_5$	0.0	69.9	30.1	1.33996(7)	–	0.55142(4)
	Pt_3Si	0.1	75.4	24.5	0.7738(7)	0.7775(6)	0.5360(2)
						$\beta = 134.02(8)^\circ$	
(Pt)+$CePt_5$+Pt_3Si	(Pt)	0.0	99.2	0.8	0.39231(4)	–	–
	$CePt_5$	16.8	83.0	0.2	0.5369(1)	–	0.4386(1)
	Pt_3Si	0.0	75.1	24.9	0.7723(2)	0.7771(1)	0.53902(7)
						$\beta = 133.85(1)^\circ$	
τ_1+τ_2+$CePt_5$	τ_1	8.1	62.0	29.9	1.6883(7)	–	–
	τ_2	9.3	72.0	18.7	Unknown	–	–
	$CePt_5$	16.0	77.7	6.3	0.5365(2)	–	0.4371(3)
τ_1+τ_4+$CePt_5$	τ_1	8.9	62.8	28.3	1.6866(1)	–	–
	τ_4	17.9	71.1	11.0	Unknown	-	–
	$CePt_5$	16.4	75.0	8.6	0.5348(6)	–	0.4364(5)

Table 2 (*continued*)

Three phase field	Phase	EPMA			Lattice parameters (nm)		
		Ce	Pt	Si	*a*	*b*	*c*
$\tau_1+\tau_3+\tau_8$	τ_1	8.6	61.6	29.8	1.6880(1)	–	–
	τ_3	15.2	54.0	30.8	1.9630(3)	0.40382(7)	1.1225(2)
	τ_8	19.6	59.7	20.5	0.40809(9)	–	0.5456(2)
$\tau_1+\tau_3+\tau_7$	τ_1	8.0	61.7	30.3	1.68760(4)	–	–
	τ_3	15.2	53.8	31.0	1.9620(3)	0.40425(7)	1.1216(3)
	τ_7	19.8	40.3	39.7	0.42580(3)	–	0.97991(9)
$\tau_3+\tau_7+\tau_8$	τ_3	15.4	54.1	30.5	1.9630(2)	0.40346(5)	1.1212(1)
	τ_7	19.3	41.7	38.8	0.42550(3)	–	0.98033(9)
	τ_8	20.5	59.3	20.2	0.4084(1)	–	0.5443(2)
$\tau_{11}+\tau_7+\tau_8$	τ_{11}	23.9	51.2	24.7	0.4099(3)	1.811(2)	0.4168(3)
	τ_7	19.9	40.1	39.9	0.42539(3)	–	0.98041(8)
	τ_8	19.9	60.4	19.6	0.4088(1)	–	0.5439(2)
$\tau_{11}+\tau_8+CePt_2$	τ_{11}	24.2	50.8	24.8	0.4100(1)	1.8085(9)	0.4185(2)
	τ_8	19.7	59.8	20.4	0.40854(8)	–	0.5449(2)
	$CePt_2$	30.3	69.2	0.5	0.77310(8)	–	–
$\tau_{11}+\tau_{16}+CePt_2$	τ_{11}	25.3	49.7	25.0	0.4106(4)	1.799(2)	0.4183(4)
	τ_{16}	33.2	55.6	11.2	0.7391(4)	1.2959(9)	0.7725(4)
	$CePt_2$	31.9	67.9	0.2	0.77286(3)	–	–
$\tau_{11}+\tau_{15}+\tau_{16}$	τ_{11}	25.7	49.2	25.1	0.4093(2)	1.801(2)	0.4192(3)
	τ_{15}	33.0	45.5	21.5	Unknown	–	–
	τ_{16}	33.1	55.4	11.5	0.739(1)	1.296(1)	0.751(1)
$\tau_{11}+\tau_{14}+\tau_{15}$	τ_{11}	24.6	50.5	24.8	0.4102(1)	1.8047(5)	0.4191(2)
	τ_{14}	32.8	33.9	33.3	0.4204(2)	–	1.4496(9)
	τ_{15}	32.6	45.4	22.0	Unknown	–	–
$\tau_{11}+\tau_{14}+\tau_7$	τ_{11}	24.6	50.6	24.8	0.4104(3)	1.808(2)	0.4163(3)
	τ_{14}	32.5	34.6	32.9	0.4202(2)	–	1.446(2)
	τ_7	19.8	41.2	38.9	0.42550(3)	–	0.9795(1)
$\tau_{13}+\tau_{14}+\tau_7$	τ_{13}	33.6	22.4	44.0	0.41560(1)	–	0.42535(8)
	τ_{14}	33.2	26.7	40.1	0.41875(5)	–	1.4490(2)
	τ_7	20.1	38.9	41.0	0.42551(3)	–	0.9797(1)
$\tau_{13}+\tau_6+\tau_7$	τ_{13}	33.1	19.3	47.6	0.4117(2)	–	0.4304(2)
	τ_6	20.1	33.7	46.2	0.9957(7)	1.1627(5)	0.5985(3)
	τ_7	19.9	37.7	42.4	0.42474(7)	–	0.9830(2)
$\tau_{10}+\tau_{13}+\tau_6$	τ_{10}	25.1	24.5	50.4	0.42908(3)	1.6739(2)	0.42371(5)
	τ_{13}	33.4	17.8	48.8	0.4129(1)	–	0.4299(1)
	τ_6	20.0	32.1	47.9	–	–	–
$\tau_{10}+\tau_{13}+CeSi_2$	τ_{10}	24.8	25.1	50.1	0.42984(5)	1.6722(2)	0.42295(7)
	τ_{13}	32.7	13.9	53.4	0.40992(7)	–	0.43149(8)
	$CeSi_2$	33.3	9.9	56.8	0.4205(2)	–	1.4082(7)
$\tau_{13}+CeSi+CeSi_2$	τ_{13}	34.3	12.5	53.2	0.40960(4)	–	0.43130(3)
	CeSi	49.8	0.0	50.2	0.8296(1)	0.39648(4)	0.59597(5)
	$CeSi_2$	~34	~8	~58	0.41807(5)	–	1.4054(3)
$\tau_{13}+\tau_{17}+CeSi$	τ_{13}	33.8	19.5	46.7	0.41403(5)	–	0.42804(4)
	τ_{17}	43.3	13.9	42.8	0.4102(1)	0.43261(1)	1.8346(5)
	CeSi	50.0	0.0	50.0	0.82905(9)	0.39711(4)	0.59582(6)
$\tau_{17}+Ce_5Si_4+CeSi$	τ_{17}	43.5	13.9	42.5	0.41023(6)	0.43265(5)	1.8341(2)
	Ce_5Si_4	55.6	1.0	43.4	0.79525(7)	–	1.5047(2)
	CeSi	50.1	3.7	46.2	0.8254(1)	0.39997(7)	0.59452(9)
$\tau_{17}+\tau_{18}+Ce_5Si_4$	τ_{17}	43.0	14.0	42.9	0.41035(9)	0.4322(4)	1.8399(5)
	τ_{18}	55.5	6.7	37.8	0.7704(2)	1.5321(4)	0.8000(3)
	Ce_5Si_4	55.6	4.6	39.8	0.79669(6)	–	1.4948(2)

Table 2 (*continued*)

Three phase field	Phase	EPMA			Lattice parameters (nm)		
		Ce	Pt	Si	*a*	*b*	*c*
Ce_3Si_2+Ce_5Si_3+Ce_5Si_4	Ce_3Si_2	59.6	4.2	36.2	0.778746)	–	0.43824(6)
	Ce_5Si_3	62.3	5.6	32.1	0.78581(3)	–	1.3872(5)
	Ce_5Si_4	55.8	4.2	40.1	0.7977(5)	–	1.499(3)
Ce_5Si_3+Ce_7Pt_3+*L*	Ce_5Si_3	~63	~7	~30	0.7869(2)	–	1.3799(6)
	Ce_7Pt_3	70.2	25.1	4.7	1.0251(2)	–	0.6380(2)
	L	–	–	––	–	–	–
τ_{19}+Ce_3Pt_2+Ce_5Si_3	τ_{19}	54.9	30.8	14.3	Unknown	–	–
	Ce_3Pt_2	60.5	36.9	2.6	0.8976(2)	–	1.7124(3)
	Ce_5Si_3	61.4	11.2	27.4	0.7855(2)	–	1.3850(5)
τ_{19}+Ce_3Pt_2+CePt	τ_{19}	55.2	34.7	10.1	Unknown	–	–
	Ce_3Pt_2	–	–	–	0.896(1)	–	1.711(2)
	CePt	49.5	46.1	4.4	0.3941(2)	1.0899(5)	0.4518(2)
τ_{17}+τ_{18}+CePt	τ_{17}	42.6	14.8	42.6	0.41055(6)	0.43222(8)	1.8339(3)
	τ_{18}	55.2	12.9	31.9	0.7643(1)	1.5330(3)	0.8007(2)
	CePt	49.8	45.8	4.5	0.3960(1)	1.0929(2)	0.4498(2)
τ_{14}+τ_{17}+CePt	τ_{14}	33.3	32.2	34.5	0.41998(4)	–	1.4481(2)
	τ_{17}	42.9	14.9	42.1	0.41065(5)	0.43221(5)	1.8375(3)
	CePt	49.7	44.3	6.0	0.3974(1)	1.0940(4)	0.4479(1)
τ_{13}+τ_{14}+τ_{17}	τ_{13}	33.3	22.3	44.4	0.41563(8)	–	0.42576(7)
	τ_{14}	33.4	26.5	40.1	0.41856(3)	–	1.4481(1)
	τ_{17}	42.9	14.9	42.2	0.4110(5)	0.4320(3)	1.8359(7)
τ_{14}+τ_{15}+CePt	τ_{14}	33.0	33.6	33.4	0.4206(1)	–	1.4490(3)
	τ_{15}	33.3	44.4	22.3	Unknown	–	–
	CePt	50.1	48.5	1.4	0.3919(1)	1.0929(5)	0.4532(1)
τ_{15}+τ_{16}+CePt	τ_{15}	32.9	45.7	21.4	Unknown	–	–
	τ_{16}	32.9	56.5	10.6	0.74025(8)	1.2951(2)	0.7508(7)
	CePt	48.8	49.5	1.7	0.3944(9)	1.090(2)	0.4531(7)
τ_{16}+Ce_3Pt_4+CePt	τ_{16}	33.5	55.5	11.0	0.7393(2)	1.2947(2)	0.7512(2)
	Ce_3Pt_4	43.1	56.7	0.2	1.3661(7)	–	0.5779(3)
	CePt	48.9	50.2	0.9	0.3934(3)	1.0893(7)	0.4531(2)
τ_{16}+Ce_3Pt_4+$CePt_2$	τ_{16}	33.6	55.5	10.9	0.7393(3)	1.2946(5)	0.7512(3)
	Ce_3Pt_4	42.2	57.5	0.3	1.3662(8)	–	0.5780(4)
	$CePt_2$	33.7	66.1	0.2	0.77270(3)	–	–

the Gd_5Si_4-type branch of the Sm_5Ge_4-type of structure. Results of the refinement for $Ce_5(Pt_{0.12}Si_{0.88})_4$, which converged to $R_{F^2} = 0.037$ with residual electron densities smaller than $\pm 3.7\,e^-/10^{-3}\,nm^3$, are summarized in Table 3.

4.2.2. The crystal structure of τ_3-$Ce_2Pt_7Si_4$

The phase field $\tau_1(Ce_3Pt_{23}Si_{11})$–$\tau_7(CePt_{2-x}Si_{2+x})$–$\tau_8(CePt_3Si)$ was found to contain a new powder spectrum from a compound with practically no homogeneity region centered around composition $Ce_{15.3}Pt_{54.0}Si_{30.7}$ (in at%, from EPMA). The intensity pattern of a single crystal, isolated from the alloy $Ce_{15.4}Pt_{54.1}Si_{30.5}$, was indexed with an orthorhombic symmetry, i.e., space group *Pnma* and lattice parameters: $a = 1.96335(8)\,nm$, $b = 0.40361(4)\,nm$, $c = 1.12240(6)\,nm$. Direct methods yielded a completely ordered atom arrangement isotypic with the structure type of $Ce_2Pt_7Ge_4$ [36]. Results of the refinement for $Ce_2Pt_7Si_4$, which converged to $R_{F^2} = 0.029$ with residual electron densities smaller than $\pm 5.9\,e^-/10^{-3}\,nm^3$, are summarized in Table 3. The composition derived from the refinement is in perfect agreement with EPMA.

4.2.3. The crystal structure of τ_{10}-$CePtSi_2$

Although the crystal structure of $CeNiSi_2$ has been elucidated in several representatives [36], the X-ray intensity pattern of a single crystal, isolated from the alloy $Ce_{25}Pt_{25}Si_{50}$, was studied (space group *Cmcm* and lattice parameters: $a = 0.42943(2)\,nm$, $b = 1.67357(5)\,nm$, $c = 0.42372(2)\,nm$). From direct methods a completely ordered atom arrangement was prompted being isotypic with the structure type of $CeNiSi_2$. No site defects were observed. The refinement converged to $R_{F^2} = 0.021$ with residual electron densities smaller than $\pm 7.6\,e^-/10^{-3}\,nm^3$ (see Table 3).

4.2.4. Rietveld refinement of Pt_3Si

For Pt_3Si, two polymorphic modifications (Fe_3C-type [44] and Pt_3Ge-type [42]) are reported in the literature. However, Pt_3Si in as-cast state and after annealing at 800 °C showed an X-ray powder diffraction pattern incompatible with the Fe_3C-type structure, which was reported for ht-Pt_3Si [44] and was suggested to exist in the temperature range from 440 to 876 °C [41]. The structure data presented for rt-Pt_3Si (Pt_3Ge-type, space group

Table 3
X-ray single-crystal data at RT for various compounds from the Ce–Pt–Si system (Mo $K\alpha$ radiation); structure data are standardized with program *Structure Tidy* [36]

Compound	$Ce_5(Pt_xSi_{1-x})_4$	$Ce_2Pt_7Si_4$	$CePtSi_2$
Nominal composition (at%)	$Ce_{55.6}Pt_{8.0}Si_{36.4}$	$Ce_{16}Pt_{54}Si_{30}$	$Ce_{25}Pt_{25}Si_{50}$
Formula from X-ray refinement in at%	$Ce_5(Pt_xSi_{1-x})_4$, $x = 0.12$	$Ce_2Pt_7Si_4$	$CePtSi_2$
	$Ce_{55.5}Pt_{5.3}Si_{39.2}$	$Ce_{15.4}Pt_{53.8}Si_{39.2}$	$Ce_{25}Pt_{25}Si_{50}$
Crystal size (mkm)	$54 \times 70 \times 80$	$54 \times 54 \times 27$	$27 \times 27 \times 54$
Structure type	Sm_5Ge_4 (branch Gd_5Si_4)	$Ce_2Pt_7Ge_4$	$CeNiSi_2$
Space group	*Pnma*	*Pnma*	*Pnma*
Lattice parameters (nm)	$a = 0.77223(3)$	$a = 1.96335(8)$	$a = 0.42943(2)$
	$b = 1.53279(8)$	$b = 0.40361(4)$	$b = 1.67357(5)$
	$c = 0.80054(5)$	$c = 1.12240(6)$	$c = 0.42372(2)$
μ_{abs} (mm^{-1})	38.51	120.10	61.11
Data collection, 2Θ range (°)	$2 \leqslant 2\Theta \leqslant 72.6$; 75 s/frame	$2 \leqslant 2\Theta \leqslant 72.6$; 150 s/frame	$2 \leqslant 2\Theta \leqslant 72.6$; 220 s/frame
Total number of frames	356, 5 sets	400, 5 sets	523, 7 sets
Reflections in refinement	$1800 \geqslant 4\sigma(F_0)$ of 2238	$2058 \geqslant 4\sigma(F_0)$ of 2376	$428 \geqslant 4\sigma(F_0)$ of 440
Mosaicity	0.45	0.50	0.55
Number of variables	53	80	18
$R_{F^2} = \Sigma\lvert F_0^2 - F_c^2\rvert / \Sigma F_0^2$	0.037	0.029	0.021
R_{Int}	0.062	0.065	0.067
wR_2	0.109	0.90	0.056
GOF	1.111	1.192	1.259
Extinction (Zachariasen)	0.0002(1)	0.00068(4)	0.0015(2)
Atom site 1	Ce1 in 8*d* (*x*,*y*,*z*)	Ce1 in 4*c* $(x, \frac{1}{4}, z)$	Ce1 in 4*c* $(0, y, \frac{1}{4})$
	0.31321(5), 0.12119(2), 0.18026(4)	0.21910(4), 0.51894(7)	0.39465(3)
Occ.	1.00(1)	1.00(1)	1.00(1)
U_{11},U_{22},U_{33} (in $10^2\,nm^2$)	0.0151(2), 0.0133(2),0.0146(2)	0.0071(3), 0.0075(3),0.0052(3)	0.0035(2),0.0038(2), 0.0045(2)
U_{23},U_{13},U_{12} (in $10^2\,nm^2$)	0.0003(1), 0.0011(1), 0.0005(1)	$U_{23} = U_{12} = 0$, $U_{13} = -0.0019(2)$	$U_{23} = U_{13} = U_{12} = 0.0$
Atom site 2	Ce2 in 8*d* (*x*,*y*,*z*)	Ce2 in 4*c* $(x, \frac{1}{4}, z)$	Pt1 in 4*c* $(0, y, \frac{1}{4})$
	0.03037(5), 0.59774(3), 0.18278(4)	0.02914 (4), 0.74378(6)	0.18004(2)
Occ.	1.00(1)	1.00(1)	1.00(1)
U_{11},U_{22},U_{33} (in $10^2\,nm^2$)	0.0159(2), 0.0172(2), 0.0145(2)	0.0055(3), 0.0066(3),0.0026(3)	0.0043(1),0.0044(1), 0.0048(2)
U_{23},U_{13},U_{12} (in $10^2\,nm^2$)	0.0026(1), 0.0022(1), 0.0036(1)	$U_{23} = U_{12} = 0$, $U_{13} = 0.0008(2)$	$U_{23} = U_{13} = U_{12} = 0.0$
Atom site 3	Ce3 in 4*c* $(x, \frac{1}{4}, z)$	Pt1 in 4*c* $(x, \frac{1}{4}, z)$	Si1 in 4*c* $(0, y, \frac{1}{4})$
	0.14248(8), 0.51233(7)	0.21227(3), 0.19866 (5)	0.7495(1)
Occ.	1.00(1)	1.00(1)	1.00(1)
U_{11},U_{22},U_{33} (in $10^2\,nm^2$)	0.0266(3), 0.0171(3), 0.0232(3)	0.0046(2), 0.0083(2),0.0082(2)	0.0044(8),0.0046(7), 0.0046(8)
$U_{23} = U_{12} = 0$, U_{13} (in $10^2\,nm^2$)	0.0004(2)	−0.0022(2)	$U_{23} = U_{13} = U_{12} = 0.0$
Atom site 4	M1 in 8*d* (*x*,*y*,*z*)	Pt2 in 4*c* $(x, \frac{1}{4}, z)$	Si2 in 4*c* $(0, y, \frac{1}{4})$
	0.13940(15), 0.04027(8), 0.47641(14)	0.03354(3), 0.06290(5)	0.0359(1)
Occ.	0.114(2)Pt+0.886(2) Si	1.00(1)	1.00(1)
U_{11},U_{22},U_{33} (in $10^2\,nm^2$)	0.0213(6), 0.0179(5), 0.0163(5)	0.0041(2), 0.0063(2),0.0035(2)	0.0060(8),0.0025(6), 0.0034(9)
U_{23},U_{13},U_{12} (in $10^2\,nm^2$)	0.0032(4), −0.0005(4), −0.0029(4)	$U_{23} = U_{12} = 0$, $U_{13} = -0.0001(2)$	$U_{23} = U_{13} = U_{12} = 0.0$
Atom site 5	M2 in 4*c* $(x, \frac{1}{4}, z)$	Pt3 in 4*c* $(x, \frac{1}{4}, z)$	
	0.0201(2), 0.0973(2)	0.65850(3), 0.55722 (5)	
Occ.	0.152(2) Pt+0.848 Si	1.00(1)	
U_{11},U_{22},U_{33} (in $10^2\,nm^2$)	0.0111(6), 0.0155(6), 0.0143(6)	0.0059(2), 0.0070(2),0.0040(2)	
$U_{23} = U_{12} = 0$, U_{13} (in $10^2\,nm^2$)	0.0010(4)	−0.0012(2)	
Atom site 6	M3 in 4*c* $(x, \frac{1}{4}, z)$	Pt4 in 4*c* $(x, \frac{1}{4}, z)$	
	0.2528(2), 0.8784(2)	0.37290(3), 0.62011 (5)	
Occ.	0.096(2) Pt+0.904 Si	1.00(1)	
U_{11},U_{22},U_{33} (in $10^2\,nm^2$)	0.0141(8), 0.0153(7), 0.0129(7)	0.0061(2), 0.0066(2),0.0027(2)	
$U_{23} = U_{12} = 0$, U_{13} (in $10^2\,nm^2$)	−0.0005(5)	0.0010(2)	
Atom site 7		Pt5 in 4*c* $(x, \frac{1}{4}, z)$	
		0.04156 (3), 0.45063(5)	
Occ.		1.00(1)	
U_{11},U_{22},U_{33} (in $10^2\,nm^2$)		0.0054(2), 0.0064(2),0.0040(2)	
$U_{23} = U_{12} = 0$, U_{13} (in $10^2\,nm^2$)		0.0009(2)	
Atom site 8		Pt6 in 4*c* $(x, \frac{1}{4}, z)$	
		0.36574 (3), 0.86767 (5)	
Occ.		1.00(1)	
U_{11},U_{22},U_{33} (in $10^2\,nm^2$)		0.0071(2), 0.0085(2),0.0024(2)	
$U_{23} = U_{12} = 0$, U_{13} (in $10^2\,nm^2$)		−0.0004(21))	
Atom site 9		Pt7 in 4*c* $(x, \frac{1}{4}, z)$	
		0.34850 (3), 0.24305 (5)	
Occ.		1.00(1)	
U_{11},U_{22},U_{33} (in $10^2\,nm^2$)		0.0046(2), 0.0162(2),0.0043(2)	
$U_{23} = U_{12} = 0$, U_{13} (in $10^2\,nm^2$)		−0.0006(2)	
Atom site 10		Si1 in 4*c* $(x, \frac{1}{4}, z)$; 0.2446(2), 0.7976(4)	

Table 3 (*continued*)

Compound	$Ce_5(Pt_xSi_{1-x})_4$	$Ce_2Pt_7Si_4$	$CePtSi_2$
Occ.		1.00(1)	
U_{11},U_{22},U_{33} (in 10^2 nm^2)		0.007(2), 0.009(2),0.003 (2)	
$U_{23}=U_{12}=0$, U_{13} (in 10^2 nm^2)		0.0014(12)	
Atom site 11		Si2 in 4*c* $(x,\frac{1}{4},z)$	
		0.4131(2), 0.0615 (3)	
Occ.		1.00(1)	
U_{11},U_{22},U_{33} (in 10^2 nm^2)		0.004 (1), 0.006 (2),0.003 (1)	
$U_{23}=U_{12}=0$, U_{13} (in 10^2 nm^2)		0.0005(11)	
Atom site 12		Si3 in 4*c* $(x,\frac{1}{4},z)$	
		0.4136 (2), 0.4245(4)	
Occ.		1.00(1)	
U_{11},U_{22},U_{33} (in 10^2 nm^2)		0.003 (1), 0.008 (2),0.002 (1)	
$U_{23}=U_{12}=0$, U_{13} (in 10^2 nm^2)		0.0005(12)	
Atom site 13		Si4 in 4*c* $(x,\frac{1}{4},z)$	
		0.0933 (2), 0.2515(3)	
Occ.		1.00(1)	
U_{11},U_{22},U_{33} (in 10^2 nm^2)		0.007(2), 0.006 (2),0.003(2)	
$U_{23}=U_{12}=0$, U_{13} (in 10^2 nm^2)		0.001 (1)	
Residual density; e/10^{-3} nm^3 max; min	3.67; −3.02	5.37; −5.87	7.67; −2.71
Principal mean square atomic displacements of U_{ij}	Ce1 0.0161 0.0138 0.0131	Ce1 0.0082 0.0075 0.0040	Ce1 0.0045 0.0038 0.0035
	Ce2 0.0218 0.0130 0.0129	Ce2 0.0065 0.0055 0.0026	Pt1 0.0048 0.0044 0.0043
	Ce3 0.0266 0.0231 0.0171	Pt1 0.0092 0.0083 0.0036	Si1 0.0046 0.0046 0.0044
	M1 0.0236 0.0183 0.0136	Pt2 0.0063 0.0041 0.0035	Si2 0.0060 0.0034 0.0025
	M2 0.0155 0.0145 0.0108	Pt3 0.0070 0.0065 0.0035	
	M3 0.0153 0.0143 0.0127	Pt4 0.0066 0.0063 0.0024	
		Pt5 0.0064 0.0058 0.0036	
		Pt6 0.0085 0.0071 0.0024	
		Pt7 0.0162 0.0050 0.0039	
		Si1 0.0087 0.0073 0.0026	
		Si2 0.0062 0.0042 0.0027	
		Si3 0.0084 0.0036 0.0023	
		Si4 0.0072 0.0059 0.0026	

Table 4
Crystallographic data for Pt_3Si, Ce_3Pt_5Si (τ_{16}) and Ce_3PtSi_3 (τ_{17}) (X-ray powder diffraction, data at RT from image plate, Cu $K\alpha1$ radiation); standardized with program *Structure Tidy* [36]

Parameter/compound	Pt_3Si	Ce_3Pt_5Si (τ_{16})	Ce_3PtSi_3 (τ_{17})
Space group, prototype	*C*2/*m*, Pt_3Ge	*Imma*, Ce_3Pd_5Si	*Immm*, $Ba_3Al_2Ge_2$
Composition, EMPA	$Pt_{75.0}Si_{25.0}$	$Ce_{32.9}Pt_{55.6}Si_{10.6}$	$Ce_{42.8}Pt_{15.1}Si_{42.1}$
Composition from refinement	$Pt_{75.0}Si_{25.0}$	$Ce_{33.3}Pt_{55.5}Si_{11.1}$; Ce_3Pt_5Si	$Ce_{42.9}Pt_{14.6}Si_{42.5}$; $Ce_3Pt_{1.02}Si_{2.98}$
Lattice parameters (nm), (Ge standard)	$a=0.7724(2)$	$a=0.74025(8)$	$a=0.41065(5)$
	$b=0.7767(2)$, $\beta=133.86(2)^\circ$	$b=1.2951(2$)	$b=0.43221(5)$
	$c=0.5390(2)$	$c=0.7508(1)$	$c=1.8375(3)$
Reflections measured	147	247	138
2Θ range	$8\leqslant 2\Theta\leqslant 100$	$8\leqslant 2\Theta\leqslant 100$	$8\leqslant 2\Theta\leqslant 100$
Number of variables	24	25	36
$R_F=\Sigma\lvert F_0-F_c\rvert/\Sigma F_0$	0.098	0.043	0.043
$R_I=\Sigma\lvert I_0-I_c\rvert/\Sigma I_0$	0.089	0.060	0.052
$R_{wp}=[\Sigma w_i\lvert y_{0i}-y_{ci}\rvert^2/\Sigma w_i\lvert y_{0i}\rvert^2]^{1/2}$	0.074	0.047	0.037
$R_p=\Sigma\lvert y_{0i}-y_{ci}\rvert/\Sigma\lvert y_{0i}\rvert$	0.058	0.036	0.030
$R_e=[(N-P+C)/\Sigma w_i y_{0i}{}^2)]^{1/2}$	0.022	0.016	0.020
$\chi^2=(R_{wp}/R_e)^2$	11.8	8.82	3.37
Atom parameters			
Ce1	–	4 Ce1: 4*e* $(0,\frac{1}{4},z)$	2 Ce1: 2*a* (0,0,0)
		0.6393(3)	
B_{iso} (10^2 nm^2)	–	0.25(5)	1.34(3)
Ce2	–	8 Ce2: 8*h* (0,*y*,*z*)	4 Ce2: 4*j* $(\frac{1}{2},0,z)$
		0.0502(1), 0.2840(2)	0.18426(3)
B_{iso} (10^2 nm^2),	–	1.94(4)	1.88(2)
M	4 Pt1: 4*i* (*x*,0,*z*)	4 Pt1: 4*c* $(\frac{1}{4},\frac{1}{4},\frac{1}{4})$	4M:2.05(1)Pt+1.95(1)Si: 4*i* (0,0,*z*)
	0.2843(2), 0.6325(3)		0.43564(4)
B_{iso} (10^2 nm^2)	0.98(3)	2.71(6)	1.71(2)
Pt2	4 Pt2: 4*h* $(0,y,\frac{1}{2})$	16 Pt2: 16*j* (*x*,*y*,*z*)	–
	0. 2742(2)	0.2006(1), 0.60806(7), 0.0654 (2)	–
B_{iso} (10^2 nm^2)	0.9(3)	2.17(2)	–

Table 4 (*continued*)

Parameter/compound	Pt_3Si	Ce_3Pt_5Si (τ_{16})	Ce_3PtSi_3 (τ_{17})
Pt3	4 Pt3: 4*g* (0,*y*,0)	–	–
	0.1870(2)	–	–
B_{iso} (10^2 nm^2)	0.56(3)	–	–
Si1	4 Si1: 4*i* (*x*,0,*z*)	4 Si1: 4*e* (0, $\frac{1}{4}$, *z*)	4 Si1: 4*j* (0, $\frac{1}{2}$, *z*)
	0.292(2), 0.061(2)	0.037(2)	0.3604(2)
B_{iso} (10^2 nm^2)	2.1(2)	3.2(3)	2.70(9)

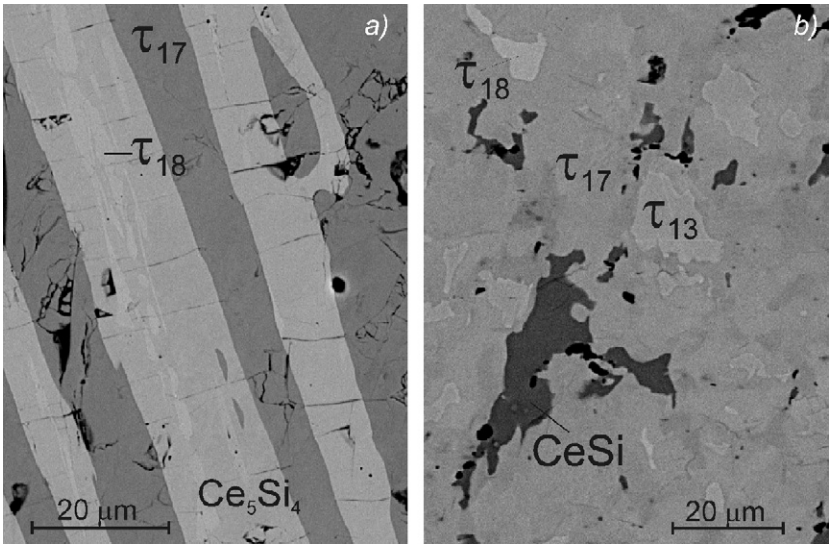

Fig. 2. Microstructure of Ce–Pt–Si alloys annealed at 800 °C: (a) $Ce_{53}Pt_7Si_{40}$ and (b) $Ce_{43}Pt_{14}Si_{40}$.

*C*2/*m* [42]) resulted in poor reliability factors, $R_F^2 = 0.266$ and $R_I = 0.396$. But further Rietveld refinement of the atomic positions arrived at satisfactorily low residual values $R_F^2 = 0.098$ and $R_I = 0.089$ (for results see Table 4).

4.2.5. *Rietveld refinement of τ_{16}-Ce_3Pt_5Si*

EPMA of alloy $Ce_{33.3}Pt_{55.6}Si_{11.1}$ (at%) annealed at 800 °C shows almost single-phase Ce_3Pt_5Si (10.6–11.2 at% Si) with a small amount of $CePt_2$. Rietveld refinement of X-ray intensities reveals complete atom order for Ce_3Pt_5Si (see Table 4), which crystallizes in the Ce_3Pd_5Si-type [47] (space group *Imma*, $a = 0.74025(8)$ nm, $b = 1.2951(2)$ nm, $c = 0.7508(1)$ nm).

4.2.6. *Rietveld refinement of τ_{17}-Ce_3PtSi_3*

The ternary compound Ce_3PtSi_3 was detected in an alloy with nominal composition $Ce_{43}Pt_{14}Si_{43}$. It forms incongruently and consequently the as-cast alloy contains significant amounts of secondary phases τ_{13}-$Ce(Pt_xSi_{1-x})_2$ and CeSi which both decompose slowly during annealing in the temperature range 800–1000 °C (Fig. 2b). Heat treatment at 800 °C for 20 days of a re-powderized and cold compacted sample reduced the amount of secondary phases to a level below 10 vol%. Rietveld refinement for Ce_3PtSi_3 yields isotypism with the structure type of $Ba_3Al_2Ge_2$ [36] (*Immm*, $Z = 2$, $a = 0.41065(5)$ nm, $b = 0.43221(5)$ nm, $c = 1.8375(3)$ nm; see Table 4). Platinum and silicon atoms randomly share the 4*i* site in a ratio 2.05:1.95. Splitting this site into two 2*a* sites (0,0,*z*) in lower symmetry (space group *Imm*2) does not support full order of the structure. Despite statistical distribution of platinum and silicon atoms in the 4*i* site of *Immm*, the compound has a limited homogeneity region at 800 °C smaller than 1 at%.

Acknowledgments

This research is supported by the Austrian National Science Foundation FWF Project P18054-Phy. The authors are grateful to the Russian Foundation of Basic Research for support of the Project nos. 08-03-01072 and 06-03-90579 BNTS and to the bilateral WTZ Austria–Russia, project 17/06.

References

[1] W.H. Lee, R.N. Shelton, Phys. Rev. B 35 (1987) 5369–5371.
[2] W.H. Lee, H.C. Ku, R.N. Shelton, Phys. Rev. B 38 (1988) 11562–11565.
[3] W.H. Lee, H.C. Ku, R.N. Shelton, Chin. J. Phys. 26 (1988) 46–53.
[4] R.N. Shelton, P. Klavins, W.H. Lee, H.C. Ku, Physica C 153–155 (1988) 447–448.
[5] B. Köhler, B. Strobel, C. Kämmerer, A. Grauel, U. Gottwick, E. Göring, A. Höhr, G. Sparn, C. Geibel, S. Horn, J. Magn. Magn. Mater. 90–91 (1990) 428–430.
[6] W.H. Lee, K.S. Kwan, P. Klavins, R.N. Shelton, Phys. Rev. B 42 (1990) 6542–6545.
[7] C. Geibel, C. Kämmerer, E. Göring, R. Moog, G. Sparn, R. Henseleit, G. Cordier, S. Horn, F. Steglich, J. Magn. Magn. Mater. 90–91 (1990) 435–437.
[8] C. Geibel, C. Kämmerer, B. Seidel, C.D. Bredl, A. Grauel, F. Steglich, J. Magn. Magn. Mater. 108 (1992) 207–208.
[9] D. Gignoux, D. Schmitt, M. Zerguine, C. Ayache, E. Bonjour, Phys. Lett. 117 (1986) 145–149.
[10] K. Hiebl, C. Horvath, P. Rogl, J. Less-Common Met. 117 (1986) 375–383.
[11] T.T.M. Palstra, A.A. Menovsky, G.J. Niewenhauys, J.A. Mydosh, J. Magn. Magn. Mater. 54–57 (1986) 435–436.
[12] C. Ayache, J. Beille, E. Bonjour, R. Calemczuk, G. Creuzet, D. Gignoux, A. Najib, D. Schmitt, J. Voiron, M. Zerguine, J. Magn. Magn. Mater. 63–64 (1987) 329–331.
[13] B.H. Grier, J.M. Lawrence, S. Horn, J.D. Thompson, J. Phys. C: Solid State Phys. 21 (1988) 1099–1110.
[14] E. Bauer, G. Hilscher, H. Michor, C. Paul, E.W. Scheidt, A.V. Gribanov, Y.D. Seropegin, H. Noël, M. Sigrist, P. Rogl, Phys. Rev. Lett. 92 (2004), 027003/1–4.
[15] E. Bauer, G. Hilscher, H. Michor, M. Siebere, E.W. Scheidt, A.V. Gribanov, Y.D. Seropegin, P. Rogl, A. Amato, W.Y. Song, J.-G. Park, D.T. Adroja, M. Nicklas, G. Sparn, M. Yogi, Y. Kitaoka, Czech. J. Phys. 54 (2004) A1–A6.

[16] S.S. Saxena, P. Mounthoux, Nature 427 (2004) 799.
[17] K.V. Samokhin, E.S. Zijlsta, S.K. Bose, Phys. Rev. B: Condens. Matter 69 (2004), 094514-1-8.
[18] M. Yogi, K. Kitaoka, S. Hashimoto, T. Yasuda, R. Settai, T.D. Matsuda, Y. Haga, Y. Onuki, P. Rogl, E. Bauer, Phys. Rev. Lett. 93 (2004), 027003/1–4.
[19] N. Tateiwa, Y. Haga, T.D. Matsuda, S. Ikeda, T. Yasuda, T. Takeuchi, R. Settai, Y. Onuki, J. Phys. Soc. Japan 74 (2005) 1903–1906.
[20] Y. Onuki, R. Settai, H. Shishido, T. Kubo, Y. Yasuda, K. Betsuyaku, H. Harima, J. Alloys Compd. 408–412 (2006) 27–32.
[21] Y. Aoki, A. Sumiyama, G. Motoyama, Y. Oda, T. Yasuda, R. Settai, Y. Onuki, J. Phys. Soc. Japan 76 (2007), 114708-1-4.
[22] J.S. Kim, D.J. Mixson, D.J. Burnette, G.R. Stewart, J. Low Temp. Phys. 147 (3–4) (2007) 135–146.
[23] T. Kawai, Y. Okuda, H. Shishido, A. Thamizhavel, T.D. Matsuda, Y. Haga, M. Nakashima, T. Takeuchi, M. Hedo, Y. Uwatoko, R. Settai, Y. Ōnuki, J. Phys. Soc. Japan 76 (2007), 014710-1-6.
[24] Y. Muro, M. Nakano, K. Motoya, Phys. B: Condens. Matter 403 (2008) 810–811.
[25] F.C. Ragel, P.V. Plessis, A.M. Strydom, J. Phys.: Condens. Matter 20 (2008), 055218-1-8.
[26] A. Gribanov, P. Rogl, in: W. Martienssen (Ed.), New Series-Landolt-Börnstein, vol. 11, Berlin, 2006, p. 356.
[27] A.V. Gribanov, Y.D. Seropegin, A.I. Tursina, O.I. Bodak, P. Rogl, H. Noël, J. Alloys Compd. 383 (2004) 286–289.
[28] A.V. Gribanov, Univ. Moscow, unpublished research, 2004.
[29] J. Emsley, The Elements, Clarendon Press, Oxford, 1991.
[30] STOE WINXPOW (Version 1.06), Stoe & Cie GmbH, Darmstadt, Germany, 1999.
[31] B.V. Nonius, Nonius, Kappa CCD Program Package: COLLECT, DENZO, SCALEPACK, SORTAV, Delft, The Netherlands, 1998.
[32] G.M. Sheldrick, Acta Crystallogr. A 46 (1990) 467–473.
[33] G.M. Sheldrick, A Computer Program for Refinement of Crystal Structures (SHELXL-97), University of Göttingen, Germany, 1997.
[34] J. Rodriguez-Carvajal, FULLPROF: a program for rietveld refinement and pattern matching analysis, in: Abstracts of the Satellite Meeting on Powder Diffraction of the XV Congress of the IUCr, Toulouse, France, 1990, p. 127.
[35] T. Roisnel, J. Rodriguez-Carvajal, in: Materials Science Forum, Proceedings of the European Powder Diffraction Conference (EPDIC7), 2000, p. 118.
[36] E. Parthé, L. Gelato, B. Chabot, M. Penzo, K. Cenzual, R. Gladyshevskii, TYPIX Standardized Data and Crystal Chemical Characterization of Inorganic Structure Types, Springer, Berlin, Heidelberg, 1994.
[37] T.B. Massalski (Ed.), Binary Alloy Phase Diagrams, second ed., ASM International, Materials Park, OH, 1990.
[38] A. Gribanov, Int. Centre for Diffraction Data, PDF-54-0563, 2003.
[39] M.V. Bulanova, P.N. Zheltov, K.A. Meleshevich, P.A. Saltykov, G. Effenberg, J. Alloys Compd. 345 (2002) 110–115.
[40] P. Schobinger-Papamantellos, K.H.J. Buschow, J. Alloys Compd. 198 (1993) 47–50.
[41] R. Massara, P. Feschotte, J. Alloys Compd. 201 (1993) 223–227.
[42] R. Gohle, R. Schubert, Z. Metallkd. 55 (1964) 503–511.
[43] W. Gold, K. Schubert, Z. Kristallogr. 128 (1969) 406–413.
[44] R.P. Ram, S. Bhan, Z. Metallkd. 69 (1978) 524–529.
[45] G. Majni, M. Costano, F. Panini, G. Celotti, J. Phys. Chem. Solids 46 (1985) 631–641.
[46] P. Villars, L.D. Calvert, Pearson's Handbook of Crystallographic Data for Intermetallic Phases, American Society for Metals, Metals Park, Ohio, 1991.
[47] A.V. Gribanov, Y.D. Seropegin, O.L. Kubarev, L.G. Akselrud, O.I. Bodak, J. Alloys Compd. 317/318 (2001) 324–326.
[48] J.M. Lawrence, Y.-C. Chen, G.H. Kwei, M.F. Hundley, J.D. Thompson, Phys. Rev. B 56 (1997) 5–8.
[49] K. Schubert, S. Bhan, W. Burkhardt, R. Gohle, H.G. Meissner, M. Pötzschke, E. Stolz, Naturwissenschaften 47 (1960) 303.
[50] E.J. Graeber, R.J. Baughman, B. Morosin, Acta Crystallogr. B 29 (1973) 1991–1994.
[51] A.I. Tursina, A.V. Gribanov, Y.D. Seropegin, K.V. Kuyukov, O.I. Bodak, J. Alloys Compd. 347 (2002) 121–123.
[52] A. Dommann, F. Hulliger, H.R. Ott, V. Gramlich, J. Less-Common Met. 110 (1985) 331–337.
[53] D. Rossi, R. Marazza, R. Ferro, J. Less-Common Met. 66 (2) (1979) P17–P25.
[54] A.I. Tursina, A.V. Gribanov, H. Noël, P. Rogl, Y.D. Seropegin, O.I. Bodak, J. Alloys Compd. 383 (2004) 239–241.
[55] S. Majumdar, E.V. Sampathkumaran, M. Brando, J. Hemberger, A. Loidl, J. Magn. Magn. Mater. 236 (2001) 99–106.
[56] K. Klepp, E. Parthe, Acta Crystallogr. B 38 (1982) 1105–1108.